ACS APPLIED MATERIALS & INTERFACES

Research Article

www.acsami.org

Photoinitiated Nitric Oxide-Releasing Tertiary *S*-Nitrosothiol-Modified Xerogels

Daniel A. Riccio, Peter N. Coneski, Scott P. Nichols, Angela D. Broadnax, and Mark H. Schoenfisch*

Department of Chemistry, University of North Carolina at Chapel Hill, Chapel Hill, North Carolina 27599, United States

Supporting Information

ABSTRACT: The synthesis of a tertiary thiol-bearing silane precursor (i.e., *N*-acetyl penicillamine propyltrimethoxysilane or NAPTMS) to enable enhanced NO storage stability at physiological temperature is described. The novel silane was co-condensed with alkoxy- or alkylalkoxysilanes under varied synthetic parameters (e.g., water to silane ratio, catalyst and solvent concentrations, and reaction time) to evaluate systematically the formation of stable xerogel films. The resulting xerogels were subsequently nitrosated to yield tertiary RSNO-modified coatings. Total NO storage ranged from 0.87 to 1.78 μmol cm^{-2} depending on the NAPTMS concentration and xerogel coating thickness. Steric hindrance near the nitroso functionality necessitated the use of photolysis to liberate NO. The average NO flux for irradiated xerogels (20% NAPTMS balance TEOS xerogel film cast using 30 μL) in physiological buffer at 37 °C was ~23 pmol cm^{-2} s^{-1}. The biomedical utility of the photoinitiated NO-releasing films was illustrated by their ability to both reduce *Pseudomonas aeruginosa* adhesion by ~90% relative to control interfaces and eradicate the adhered bacteria.

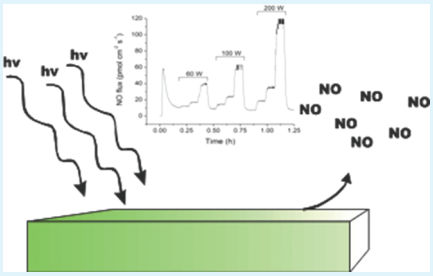

KEYWORDS: *sol–gel, antimicrobial, nitric oxide, S-nitrosothiol, photolysis*

INTRODUCTION

Reactive radical species (e.g., hydroxyl radical and superoxide) are well-suited as antimicrobial agents as their biocidal activity is broad-spectrum.[1] Such species often feature multiple mechanisms of bactericidal activity that lessen the likelihood of fostering bacterial resistance through a specific singular pathway. Light-activated antimicrobial surfaces including titanium dioxide films and photosensitizer-modified polymers represent new strategies for eliciting antibacterial activity through light-induced generation of reactive radicals and singlet oxygen.[1−4] Medical implants, catheters, and hospital-associated surfaces that are plagued by bacterial contamination would greatly benefit from the associated disinfection/sanitization capabilities of such surfaces.

Nitric oxide (NO) is another radical species with potent broad-spectrum antimicrobial activity.[5] As such, the antimicrobial utility of exogenous NO delivery via NO donors (i.e., compounds that store and release NO) has been an active area of research.[5−8] More recently, macromolecular vehicles (e.g., silica nanoparticles, metallic clusters, and dendrimers) and polymers have been functionalized with multiple NO donor moieties to enable larger reservoirs of deliverable NO.[6,9] The application of these materials as coatings provides localized NO release at a desired interface (e.g., an indwelling medical device) with effective mitigation of bacterial adhesion.[6,9] Indeed, bacteria exposed to NO-releasing surfaces exhibit impaired cellular membranes and experience lysis due to radical-induced lipid peroxidation.[10] Nevertheless, the lack of a suitable NO release trigger has limited the ultimate utility of these coatings as most formulations spontaneously liberate NO upon immersion in physiological solution.

Irradiation with light may represent a more suitable trigger for enabling both spatial and temporal control over NO release. Fortunately, NO donors susceptible to photoinitiated NO release have emerged as alternatives to *N*-diazeniumdiolate NO donors.[11,12] For example, *S*-nitrosothiols (RSNOs) are a class of NO donors capable of undergoing photolysis to release NO upon homolytic cleavage of the S−N bond (Scheme 1).[12,13]

Scheme 1. Photolytic Decomposition of *S*-Nitrosothiols to Yield Nitric Oxide

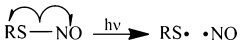

The light-initiated NO release from donors such as these has led to the development of macromolecular scaffolds and polymers with controllable NO release.[14] Specifically, silica nanoparticles,[15,16] dendrimers,[17] self-assembled monolayers,[18] polyurethanes,[19] and polyesters[20−22] have been modified with RSNO functionalities to design photoactivatable NO release vehicles. Macromolecular RSNO-bearing particles may be used as dopants within traditional polymers to fabricate photoactivated NO-releasing surfaces. Indeed, Frost and Meyerhoff doped *S*-nitroso-*N*-acetyl-DL-penicillamine (SNAP) surface-grafted silica particles into silicone rubber films at 20 wt %.[23] Although the films exhibit light-controlled NO release, total NO storage is limited at higher silica concentrations where

Received: October 19, 2011
Accepted: December 26, 2011
Published: January 18, 2012

polymer stability may be compromised resulting in undesirable particle leaching.[24]

Covalent modification of a polymer backbone with NO donor functionalities represents an alternative strategy for fabricating NO-releasing coatings with enhanced NO storage.[6,25,26] Silica-based xerogel polymers are particularly appealing as sol−gel chemistry (i.e., the hydrolysis and co-condensation of organosilanes and backbone alkoxysilanes) allows for tunable concentrations of organic functionalities to be covalently incorporated throughout the siloxane bond network.[27,28] Our laboratory has reported the use of sol−gel chemistry to prepare *N*-diazeniumdiolate-modified xerogels capable of NO release at physiological pH.[29−33] Following our initial work, we reported the synthesis of RSNO-modified xerogels using mercaptopropyl- and methyltrimethoxysilane (MPTMS and MTMOS, respectively) to provide an alternative NO release trigger.[34] Nitrosation of the covalently attached primary thiol groups yielded RSNO-modified materials that liberate NO under visible irradiation. This, coupled with optical transparency, mild synthetic conditions, inexpensive reagents, and the ability to coat many substrates suggests these materials may prove useful as photoantimicrobial surfaces. However, thermal decomposition and NO release in the dark greatly diminish the utility of these xerogels for clinical applications.

S-Nitrosothiol stability may be altered by the chemical structure of the thiol.[12] For example, tertiary RSNOs (e.g., SNAP) are more stable than their primary analogues because of steric hindrance surrounding the sulfur atom.[35,36] On the basis of this knowledge, we hypothesize that xerogels featuring tertiary derived-RSNOs may exhibit enhanced NO donor stability at physiological temperature (i.e., 37 °C). Unfortunately, tertiary thiol silanes are not readily available. The synthesis and characterization of a tertiary thiol-bearing silane was thus pursued to form more stable NO donor-modified xerogels capable of photoactivatable NO release.

EXPERIMENTAL SECTION

Materials. 3-Aminopropyltrimethoxysilane (APTMS), tetraethoxysilane (TEOS), and isobutyltrimethoxysilane (BTMOS) were purchased from Gelest (Tullytown, PA). Methyltrimethoxysilane (MTMOS) and diethylenetriamine pentaacetic acid (DTPA) were purchased from Fluka (Buchs, Switzerland). Tetramethoxysilane (TMOS) and Dulbecco's Modified Eagle's Medium (DMEM) were purchased from Sigma (St. Louis, MO). D(−)-Penicillamine, ethanol, and tetrahydrofuran (THF) were obtained from Fisher Scientific (Fair Lawn, NJ). *Pseudomonas aeruginosa* (ATCC #19143) was obtained from American Type Culture Collection (Manassas, VA). Nitric oxide calibration gas (26.8 ppm; balance N_2) was purchased from National Welders Supply Co. (Durham, NC). Type A19 60 and 100 W General Electric and type A21 200 W Sylvania incandescent light bulbs were purchased from Lowe's (Chapel Hill, NC). Tecoflex SG-80A polyurethane was a gift from Thermedics (Woburn, MA). Other solvents and chemicals were analytical-reagent grade and used as received. Distilled water was purified to 18.2 MΩ cm with a Millipore Milli-Q Gradient A-10 water purification system (Bedford, MA).

Silane and Xerogel Synthesis. *Synthesis of N-Acetyl Penicillamine (NAP) Thiolactone.* Acetic anhydride (96 mmol, 9.80 g) was added dropwise to a well stirred solution of D-(−)penicillamine (40 mmol, 5.97 g) in pyridine (50 mL) at 0 °C. After 30 min, the flask was removed from ice and allowed to stir at room temperature for 15 h. The resultant orange solution was partitioned between chloroform and dilute HCl and washed 4x with dilute HCl. After drying over $MgSO_4$, the organic phase was evaporated to yield an orange residue. The residue was first dissolved in absolute ethanol (20 mL), and then precipitated in pentane at −78 °C. The light yellow crystalline product was isolated by filtration (2.07 g, 30%). ^{1}H NMR ($CDCl_3$) δ1.65 (s, CH_3), 1.86 (s, CH_3), 2.05 (s, $NHCOCH_3$), 5.68−5.70 (d, $CHNHCOCH_3$), 6.56 ($NHCOCH_3$). ^{13}C NMR ($CDCl_3$) δ 22.52 ($NHCOCH_3$), 26.20 ($C(CH_3)_2$), 30.22 ($C(CH_3)_2$), 51.23 (CH), 169.37 ($NHCOCH_3$), 192.21 (SCO).

Synthesis of N-Acetyl Penicillamine Propyltrimethoxysilane (NAPTMS). APTMS (10 mmol, 1.78 g) was added to a stirring solution of NAP thiolactone (10 mmol, 1.72 g) in methylene chloride (20 mL). The light yellow solution was stirred for 4 h at room temperature before distillation of the methylene chloride to yield NAPTMS as a viscous clear oil. ^{1}H NMR ($CDCl_3$) δ 0.54 (t, $SiCH_2$), 1.24 and 1.39 (s, $CH(CH_3)_2SH$), 1.54 (m, $SiCH_2CH_2$), 1.96 (s, $NHCOCH_3$), 2.96 and 3.21 (m, $SiCH_2CH_2CH_2$), 3.44 (s, $Si(OCH_3)_3$), 4.63 (d, $CHC(CH_3)_2SH$), 6.99 (d, $CHNHCOCH_3$), 7.70 (t, $CH_2NHCOCH$). ^{13}C NMR ($CDCl_3$) δ 6.59 ($SiCH_2$), 22.42 and 22.97 ($CH(CH_3)_2SH$), 28.64 ($NHCOCH_3$), 30.80 ($SiCH_2CH_2$), 41.93 ($CHC(CH_3)_2SH$), 46.23 ($SiCH_2CH_2CH_2$), 50.35 ($Si(OCH_3)_3$), 60.32 ($CHC(CH_3)_2SH$), 169.64 ($CHNHCOCH_3$), 170.17 (CHCONH). Elemental analysis was performed by Midwest Microlab, LLC (Indianapolis, IN). Experimental weight percents for C, H, N, and S were 42.94, 7.75, 7.96, and 7.54, respectively, and are in agreement with the theoretical weight percents for C, H, N, and S of 44.32, 7.94, 7.95, and 9.10, respectively.

Synthesis of NAPTMS-Derived Xerogels. Xerogel coatings were prepared as follows. Sols containing 10−40 mol % NAPTMS (balance MTMOS, BTMOS, TMOS, or TEOS) were prepared by shaking ethanol (1050 μL), backbone alkylalkoxy- or alkoxysilane (86−201 μL), NAPTMS (53−210 mg; total silane molar amount = 1 mmol), water (46 μL) and 0.5 M HCl (136 μL) for 30 min−4 h. All substrates were sonicated in ethanol for 20 min, dried under N_2, and ozone (UV) cleaned for 20 min in a BioForce TipCleaner (Ames, IA) prior to casting. Aliquots of 30−120 μL were cast onto 9 × 25 mm^2 precleaned glass substrates. After casting of the sol, all physisorbed films were allowed to dry at room temperature overnight, and then transferred to a 45 °C oven for 2 days. *S*-Nitrosothiols were then formed on the room temperature-cooled films.

S-Nitrosothiol Formation. Thiols of xerogels were nitrosated by reaction with acidified nitrite. Films were protected from light and incubated for fixed intervals in solution (2 mL) containing a 100-fold molar excess of $NaNO_2$ and HCl (vs moles thiol) and 500 μM DTPA. The xerogels were washed with 500 μM DTPA and stored in the dark at −20 °C until used. Spectral characterization of RSNO formation was performed by affixing the slides normal to the light path of a PerkinElmer Lambda 40 UV/vis spectrophotometer (Norwalk, CT) in cuvettes containing 2 mL phosphate buffered saline (PBS; 10 mM phosphate, pH 7.4). Absorbance at 590 nm was monitored as a function of nitrosation reaction time and concentration of excess nitrosating agent for each composition of xerogel.

Characterization. *Nitric Oxide Release.* Nitric oxide release from RSNO-modified xerogels was monitored in 1 s intervals using a Sievers model 280i chemiluminescence nitric oxide analyzer (NOA) (Boulder, CO). Calibration of the instrument was performed prior to each experiment using 26.8 ppm NO gas (balance N_2) and air passed through a Sievers NO zero filter. Individual slides were immersed in 25 mL PBS containing 500 μM DTPA and sparged with a 200 mL/min N_2 stream. Temperature of the sample was maintained at 37 °C during irradiation by circulating thermostatted water through a custom-made flow cell. The water was circulated between the flow-cell housing the sample flask and a thermostatted water bath shielded from the lamp. Light-initiated NO release was examined by using incandescent bulbs of various wattages placed 0.6 m above the sample flask to monitor light induced fluxes and at a distance of 0.3 m without thermostatting for assaying total NO storage. The sample flask was shielded from light with aluminum foil when light was not the intended initiator of NO release.

Xerogel Film Stability. Nitrosated xerogel films on glass slides (n = 3) were immersed in 10 mL PBS and incubated at 37 °C. Films were removed and transferred to fresh solutions of PBS at fixed intervals of 6, 12, 24 h and 7 days. Silicon (Si) concentrations in the PBS soak solutions were determined using a Teledyne Leeman Laboratories Prodigy inductively coupled plasma optical emission spectrometer

(ICP-OES) (Hudson, NH) calibrated with 0−50 ppm Si standard solutions in PBS. Blank glass slides as well as slides cast with 30 μL of a 20 mg mL^{-1} polyurethane in THF solution (to examine Si leaching of glass substrates with one side coated with a polymer) were assessed as controls.

Film Thickness. Measurements of the RSNO-modified xerogels were acquired with a KLA Tencor P15 Profilometer (Milpitas, CA) at a scan speed of 100 μm s^{-1}, 200 Hz sampling rate, and a scan length of 2000 μm. Half of the RSNO-modified xerogel coating was physically removed from the glass substrate and this interface probed to acquire film thickness.

Elemental Analysis of RSNO Xerogels. The xerogel materials were analyzed for sulfur weight percent (S wt%) by Midwest Microlab, LLC (Indianapolis, IN).

Bacterial Assays. P. aeruginosa was cultured at 37 °C in tryptic soy broth (TSB), pelleted by centrifugation, resuspended in 15% glycerol (v:v in PBS), and stored at −80 °C. Cultures for bacterial adhesion studies were grown from a −80 °C stock in 37 °C TSB overnight. A 1 mL aliquot of overnight culture was inoculated into 100 mL of fresh TSB, incubated at 37 °C with rotation, and grown to a concentration of 1 × 10^8 colony forming units (cfu) mL^{-1} (verified by 10-fold serial dilutions in PBS, plating on tryptic soy agar nutrient plates, and subsequent cfu enumeration). The bacteria were pelleted by centrifugation, rinsed with ultrapure water, and resuspended in sterile PBS. Control (unnitrosated) and RSNO-modified xerogels were immersed in 4 mL aliquots of bacterial suspension and incubated at 37 °C in dark or light conditions (200 W at a distance of 0.6 m). Temperature was maintained during irradiation by circulating thermostatted water through a custom-made flow cell housing the samples. The xerogel substrates were removed from the bacterial suspension after 1 h and gently immersed in ultrapure water to dislodge loosely adhered cells. The slides were dried under a stream of N_2. To quantify bacterial adhesion, substrates were imaged in phase-contrast mode using a Zeiss Axiovert 200 inverted optical microscope (Chester, VA) at 20X magnification. Digital micrographs were captured with a Zeiss Axiocam digital camera (Chester, VA) and digitally processed to differentiate adhered cells from background. The darkened pixels, corresponding to adhered bacteria, were digitally enumerated with the extent of bacterial adhesion reported as the percent of the xerogel substrate surface covered with bacterial cells. The viable (still alive) bacteria adhered to the xerogel were determined by swabbing the nonxerogel-coated side of the slide with 70% EtOH and PBS to remove/kill adhered bacteria and residual EtOH, respectively. The slide was then placed in 4 mL of sterile PBS and bacteria adhered to the xerogel-coated side were removed from the substrate surface via sonication (40 kHz, 15 min).[37] Of note, previous work has determined that sonication under these conditions has no detriment to bacterial viability.[37] The resulting bacterial suspensions were subjected to serial 10-fold dilutions in sterile PBS, and 100 μL aliquots of each dilution were plated on tryptic soy agar (TSA) nutrient plates. The plates were incubated at 37 °C overnight and the number of live bacteria was determined by counting the number of colonies that grew on each plate overnight.

Cytotoxicity. To assess the impact of xerogel fragmentation on healthy cells, L929 murine fibroblasts were exposed directly to the xerogel fragmentation solutions. Briefly, the fibroblasts were cultivated in DMEM supplemented with 10% fetal bovine serum (v/v), 100 units penicillin, and 100 μg streptomycin, then incubated in 5% CO_2/95% air under humidified conditions at 37 °C. After attaining confluency, the cells were trypsinized and then seeded onto tissue-culture-treated polystyrene 96-well plates at a density of 1 × 10^5 cells mL^{-1}. Three days later, the media was aspirated and replaced with 1:1 dilution of the fragmentation solutions with media for 24 h viability experiments, respectively. Subsequently, the solutions were aspirated, cells were washed with sterile PBS, and 100 μL of fresh media was added to the cells. Cellular viability was assessed using the MTS assay (CellTiter 96 Aqueous Non-Radioactive Cell Proliferation Assay; Promega, Madison, WI). Briefly, the MTS reagent (20 μL) was added to each well until a purple formazan color was formed in the control (untreated) wells. The supernatant from each well was then transferred to a new 96-well plate prior to reading the absorbance at 490 nm using a Labsystems Multiskan RC microplate reader (Helsinki, Finland). Viability was expressed as a percent viability relative to cells treated to control PBS solutions.

RESULTS AND DISCUSSION

Xerogel Development. The preparation of a tertiary thiol-based silane precursor was necessary for this work as such silanes are not commercially available.[36] Penicillamine was thus reacted in the presence of acetic anhydride to prepare a NAP thiolactone in situ. After characterization by ^{1}H and ^{13}C NMR, the NAP thiolactone was coupled to APTMS resulting in a tertiary thiol-bearing silane, referred to as NAPTMS (Scheme 2). Successful synthesis of this tertiary thiol-bearing silane was verified via ^{1}H NMR characterization (see Figure S1 in the Supporting Information). Elemental analysis and ^{13}C NMR corroborated formation of the NAPTMS precursor as well.

Scheme 2. Synthesis of N-Acetylpenicillamine Propyltrimethoxysilane (NAPTMS)

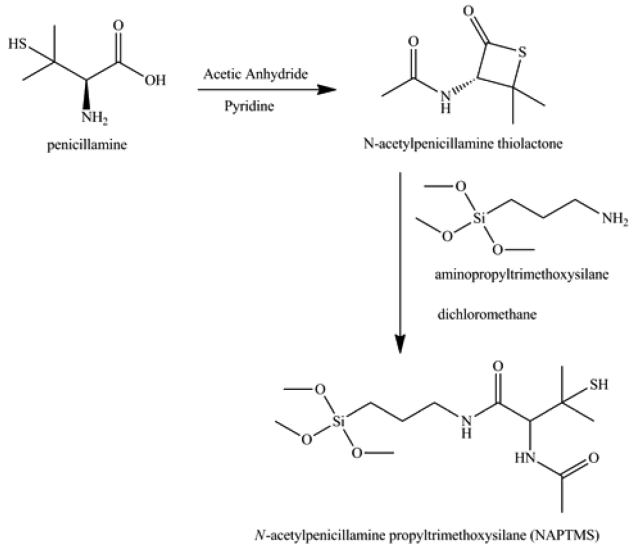

Nitric oxide-releasing xerogels are traditionally composed of organosilanes hydrolyzed and co-condensed with alkoxy- or alkylalkoxysilanes (termed "backbone silanes"). The backbone silanes impart both structural stability and tunable NO payloads by varying the silane molar ratio.[29] Unfortunately, co-condensation of silanes is not a trivial objective. Disparate hydrolysis and condensation rates between mixed silanes impact xerogel formation, and at times may prevent it altogether.[38,39] Co-condensation of NAPTMS was attempted with backbones of varying structures and reaction rates (see Figure S2 in the Supporting Information), including tetramethoxysilane (TMOS), tetraethoxysilane (TEOS), methyltrimethoxysilane (MTMOS), and isobutyltrimethoxysilane (BTMOS), to determine which composition facilitated optimal xerogel synthesis.

The compositions that proved promising (e.g., structurally stable and optically transparent) comprised combinations of NAPTMS with either MTMOS or TEOS (Scheme 3). The synthetic variables for preparing these materials included reaction times of 30−60 min, a large volume of ethanol cosolvent (1050 μL), 0.05 M HCl catalyst, a water to silane ratio of 10:1 (based on a 1 mmol total silane amount), and molar percentages of 30 mol % NAPTMS or less. Xerogel

Scheme 3. Synthesis of Tertiary Thiol-Containing Xerogel through Hydrolysis and Condensation of Silane Precursors[a]

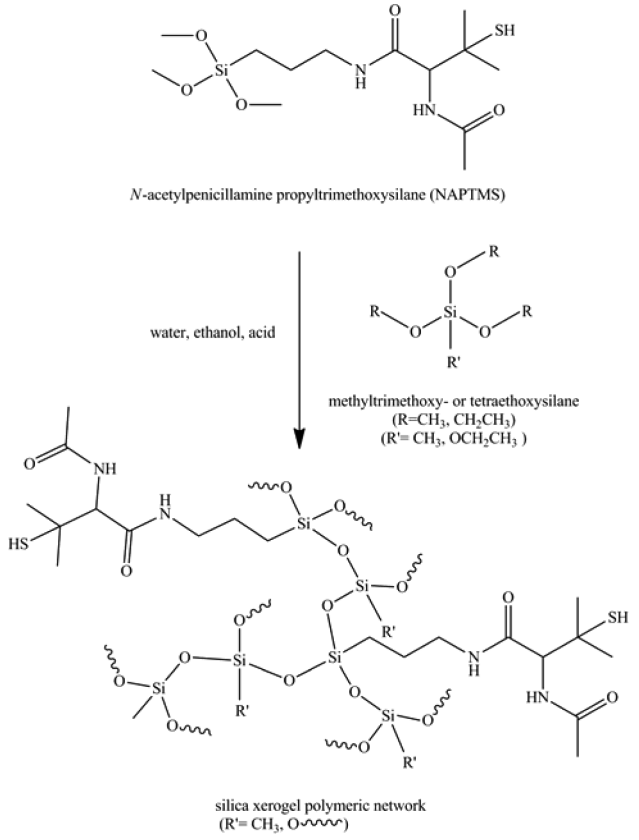

[a]The wavy bonds represent continued branching and expansion of the siloxane network. Varied possible linkages are shown to emphasize the diversity of the resulting material depending on synthetic conditions.

compositions consisting of 40 mol % NAPTMS or greater became opaque when immersed in water. Such behavior may be attributed to the presence of unreacted silicate oil within the xerogel network, leading to phase separation from reacted silanes.[40] These xerogels completely dissolved in ethanol, which also indicates the presence of unreacted silanes.[27] This incomplete xerogel formation is ostensibly due to substantial steric hindrance around the silicon atom of NAPTMS resulting in a slower condensation rate relative to MTMOS or TEOS[38,39] In turn, the NAPTMS reaction rates are not compatible with the more rapid hydrolysis/condensation reactions of the backbone silanes. Multiple synthetic parameters including the water to silane ratio and amount of acid catalyst were tuned in an attempt to remedy this problem as previous research has shown their impact on silane reaction rates.[27,41] However, traditional strategies such as altering the water to total silane ratio (1:4, 2:1, 4:1, 10:1, and 20:1) did not lead to improved stability, nor did modifications to the reaction time (0.5−5 h), acid catalyst concentration (0.01−0.20 M), catalyst type (NaOH vs HCl), ethanol solvent volume (25−1050 μL), drying time (0.25−5 days), or drying temperature (25−70 °C). For example, xerogels synthesized with greater concentrations of catalyst (e.g., 0.2 M HCl) led to nonuniform and opaque coatings with significant topographical heterogeneity. Reactions with lower catalyst concentrations (e.g., 0.01 M HCl) were not structurally sound. In the end, we concluded that the large concentration of NAPTMS (i.e., ≥40 mol %) was prohibitive for forming xerogels regardless of the other conditions varied.

With respect to other backbone silanes (i.e., TMOS and BTMOS), TMOS-derived NAPTMS xerogels fractured upon drying/curing indicating an insufficiently pliant or porous network not able to deal with stress inherent to solvent evaporation. Indeed, pressure gradients within such polymers due to solvent evaporation have been reported to result in nonuniform drying and ensuing xerogel cracking.[27,40,42] The four bridging ligands of TMOS enhance polymer cross-linking and interchain cohesion during xerogel formation, resulting in a more rigid silica network prone to such cracking. The main strategy to decrease the pressure gradient and resulting xerogel fracture is to reduce the evaporation rate.[42] Unfortunately, applying this strategy (drying at 25 °C) to NAPTMS/TMOS xerogels still led to cracking. As TMOS and MTMOS structures are similar in size and steric hindrance, successful film formation using MTMOS but failure (i.e., cracking) with TMOS suggests a reason other than reaction rate differences for this behavior. Incorporation of silane precursors with nonhydrolyzable ligands has been used previously as a viable strategy for creating more pliant networks and circumventing xerogel fracturing.[27] We believe that the one nonhydrolyzable ligand for MTMOS lessens the steric constraints and interchain cohesion within the silica network to produce films with greater integrity during/after drying.[43]

Because TMOS and TEOS exhibit similarly rigid networks, we attribute the more optimal (e.g., structurally stable) TEOS-derived films to the increased steric hindrance associated with TEOS (increased carbon chain length compared to TMOS), thereby decreasing the rate of hydrolysis and condensation of this silane under acid-catalyzed sol−gel reactions.[27,44] In this respect, the hydrolysis/condensation rates for TEOS and NAPTMS are better matched and thus facilitate successful co-condensation of the precursors, enhanced NAPTMS incorporation within the network, and greater flexibility due to the lessened interchain cohesion and rigidity. Reactions of NAPTMS with TEOS also produced films of greater integrity at shorter reaction times (i.e., 30 min vs 1 h) compared to those formed with MTMOS at shorter reaction times. If the TEOS precursor retained a large degree of unhydrolyzed ligands because of the shorter reaction time, the resulting network would be more pliant and avoid fracture upon drying.[27]

Xerogels derived from BTMOS exhibited incomplete co-condensation and xerogel formation. Although BTMOS and NAPTMS may have similarly matched reaction rates, both rates are likely too slow for adequate xerogel formation. Increasing the catalyst amount or the reaction time to promote reaction between the two silanes did not improve xerogel stability for BTMOS-based films.

Because the NAPTMS concentrations were limited to ≤30 mol %, alternative strategies were necessary to affect NO release kinetics and payloads (e.g., increasing the amount of sol cast per surface area of substrate). To evaluate the role of xerogel thickness and NAPTMS concentration on NO release, 30−120 μL aliquots of 10, 20, and 30 mol % NAPTMS compositions with either TEOS or MTMOS were cast on glass substrates. All xerogels formed from casting volumes >60 μL cracked upon drying. This behavior was expected at some upper threshold as enhanced pressure gradients are characteristic for thicker xerogel films, ultimately leading to greater fracturing upon drying.[27] Unfortunately, 10 mol % NAPTMS balance MTMOS compositions were opaque and did not

uniformly coat substrates. These films were stable in ethanol, indicating complete xerogel formation. The opacity in these instances is attributed to microsyneresis or clustering of the silica network that results in phase separation from the residual solvent.[27] Nevertheless, xerogels lacking optical transparency were considered undesirable since photoinitiated NO release is the intended application. Although 30 μL cast from a 20 mol % NAPTMS balance MTMOS composition formed glassy, homogeneous films (7.8 ± 0.9 μm), 45 and 60 μL casts were similar in opaque appearance to the 10 mol % compositions. Xerogels consisting of 30 mol % NAPTMS balance MTMOS at 30, 45, and 60 μL casting volumes formed optically transparent xerogels with resulting thicknesses of 10.0 ± 1.4, 15.4 ± 2.3, and 19.1 ± 2.1 μm, respectively.

Similarly, ideal TEOS films were formed using 20 mol % NAPTMS at 30, 45, and 60 μL casting volumes and 30% NAPTMS at 30 μL cast with corresponding thicknesses of 8.65 ± 0.81, 14.4 ± 0.3, 19.3 ± 3.3, and 10.3 ± 2.0 μm, respectively. Greater casting volumes for the 30% NAPTMS balance TEOS films exhibited cracking upon drying. Compositions derived from 10 mol % NAPTMS balance TEOS cracked upon drying as well, ostensibly due to an excessive concentration of TEOS in the silica network causing a lack of pliance within the xerogel framework. Altogether, eight stable xerogel formulations composed of NAPTMS/MTMOS and NAPTMS/TEOS as a function of silane mol % and casting volumes were subsequently pursued as novel NO-releasing photoantimicrobial surfaces.

Xerogel Nitrosation. Thiols are readily converted to NO donor form (i.e., RSNOs) by exposure to nitrosating agents such as nitrous acid (commonly generated in situ from acidified nitrite solutions).[13] *S*-Nitrosothiol formation is accompanied by a color change with primary RSNOs red in appearance and tertiary RSNOs green. Thus, characteristic RSNO absorbance bands in the UV (330–350 nm; $n_O \rightarrow \pi^*$) and visible (550–600 nm; $n_N \rightarrow \pi^*$) regions are used to monitor RSNO formation.[12] Initial UV/vis spectroscopy studies indicated that optimal nitrosation of the NAPTMS-derived films required a 100-fold molar excess of acidified nitrite. With the associated steric hindrance surrounding the tertiary thiol functionality, a large excess of acidified nitrite for nitrosation was expected.[12] The optimal nitrosation time was studied as a function of backbone and casting volume, and determined when the absorbance at 590 nm no longer increased (indicating the nitrosation had reached a maximum). As provided in the Supporting Information, the degree of nitrosation was not enhanced with reaction times >3 h (MTMOS-based films cast from 30 μL). Identical analysis revealed that thicker MTMOS-based films (regardless of NAPTMS mol %) required slightly longer reaction time (4 h), presumably due to slowed diffusion of the nitrosating agent through the coatings. In contrast, xerogels derived from TEOS reacted more rapidly, and were maximally nitrosated after 1 h incubation regardless of casting volume. The difference between TEOS and MTMOS may be attributed to TEOS's lower organic character that would facilitate more rapid penetration of the aqueous nitrosating agent into the xerogel network.

Nitric Oxide Release Characterization. Although more stable than their primary counterparts, tertiary RSNOs still undergo decomposition (and NO release) by typical RSNO pathways including thermal and photolytic-based S–NO cleavage and copper ion-mediated reduction.[12,13] Due to negligible physiological levels of "free" copper[45−47] and the intended photoinitiated release of NO from these tertiary RSNO-modified xerogels, the effect of copper on NO release was not investigated. Any trace copper in the buffer was chelated with diethylenetriamine pentaacetic acid (DTPA) prior to NO release characterization.

Photoinitiated NO release from RSNO-modified xerogels was measured using a chemiluminescence nitric oxide analyzer capable of monitoring NO in real time. Individual films were immersed in 500 μM DTPA (pH 7.4 PBS) at 37 °C. As expected, visible irradiation greatly influenced the NO release from the coatings. The NO flux from a representative xerogel film (30 mol % NAPTMS balance TEOS, 30 μL cast) increased proportionally with greater source intensity (bulb wattage) and inversely with distance between the lamp and sample flask (Figure 1). The rapid NO release kinetics associated with the

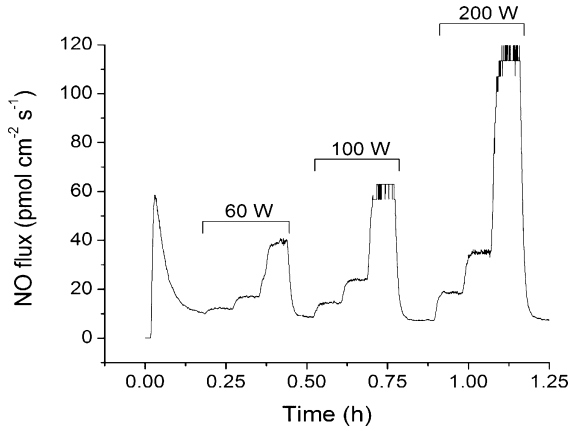

Figure 1. Nitric oxide flux from a NAPTMS xerogel (30 mol %, balance TEOS; 30 μL cast) at 37 °C under periods of light irradiation. Increasing bulb wattages are noted. Successive steps under each period of irradiation correspond to distances between the light source and sample of 0.9, 0.6, and 0.3 m.

200 W light at a distance of 0.3 m proved ideal for quantifying the total amount of NO stored within the films. A period of 16 h of irradiation under these conditions liberated all of the NO from the films as indicated by both a return to baseline on the instrument and the disappearance of the film's greenish hue.

To aid comparison among different compositions as well as to previous materials, the total NO storage of the xerogels is reported relative to the surface area of the coating and normalized per mass of deposited material. As shown in Table 1, the tertiary RSNO-modified xerogels stored 0.20–0.62 μmol NO per mg of material. Of note, the mass-normalized NO storage was not equivalent at different casting volumes of the same composition. For example, 30 mol % NAPTMS/MTMOS compositions stored 0.47 ± 0.10 μmol mg^{-1} when cast at 30 μL (~5 mg of xerogel upon drying), but only 0.28 ± 0.07 μmol mg^{-1} when 60 μL was cast (~12 mg of deposited material). Although nitrosation times were optimized for individual casting volume, this nonlinearity indicates that the extent of nitrosation may be limited by casting volume (thickness). For example, the nitrosating agent may be less accessible to thiols located within the interior of the film. Indeed, the dense structure and limited porosity of acid-catalyzed xerogels are well-known.[27]

Although thicker films stored less NO per mass of identical xerogel for all compositions, the difference was more pronounced for MTMOS-derived films. This behavior was

Table 1. Total NO Stored, Sulfur Content, and Degree of Thiol to *S*-Nitrosothiol Conversion for Tertiary RSNO-Modified Xerogels

			total NO released			
NAPTMS (mol %)	backbone	casting volume (μL)	(μmol cm^{-2})	(μmol mg^{-1})	sulfur content (weight %)	RSNO conversion efficiency (%)
20	TEOS	30	1.02 ± 0.26	0.25 ± 0.06	3.89	20.2
20	TEOS	45	1.16 ± 0.44	0.20 ± 0.08	3.89	16.9
20	TEOS	60	1.48 ± 0.29	0.24 ± 0.05	3.89	19.9
30	TEOS	30	1.78 ± 0.09	0.62 ± 0.03	5.05	39.2
20	MTMOS	30	0.87 ± 0.31	0.31 ± 0.11	2.51	39.3
30	MTMOS	30	1.13 ± 0.23	0.47 ± 0.10	4.57	32.9
30	MTMOS	45	1.22 ± 0.48	0.27 ± 0.11	4.57	19.1
30	MTMOS	60	1.64 ± 0.39	0.28 ± 0.07	4.57	19.9

somewhat expected as these films also required different nitrosation times depending on the casting volume, whereas TEOS-based films reached optimal nitrosation at equivalent times regardless of casting volume.

Despite the variation in NO storage per mass, a correlation between xerogel thickness an NAPTMS mol % was noted when the total NO storage was normalized to the surface area of the coating (Table 1). Increasing either the thickness or NAPTMS concentration of the coating enhanced the NO storage to 0.87 to .78 μmol cm^{-2}. When comparing equivalent NAPTMS concentrations and casting volumes, the TEOS-based films stored more NO than MTMOS-based films. The large reservoirs of NO stored within these materials are comparable to previously reported NO-releasing xerogels capable of both reducing bacterial adhesion[31−34,48] and implant-associated infection,[49] and mitigating the foreign body response,[50] illustrating the biomedical potential of these tertiary RSNO-modified xerogels.

To confirm that the degree of nitrosation varied for each composition, we used elemental analysis of the films to deduce the amount of sulfur in the xerogels. As shown in Table 1, 20 mol % NAPTMS balance TEOS films were characterized as having 3.89 wt % sulfur while the equivalent MTMOS counterpart contained 2.51 wt %. Likewise, the sulfur concentrations in 30 mol % NAPTMS xerogels were 5.05 and 4.57 wt % when formed with TEOS and MTMOS, respectively. As shown in Table 1, the nitrosation efficiencies for 20 mol % NAPTMS/TEOS films were ∼17−20% regardless of casting volume. Increasing the NAPTMS concentration to 30 mol % resulted in a greater nitrosation efficiency (∼39%), suggesting that higher thiol incorporation increases thiol accessibility to the nitrosating agent (i.e., more thiols are nearer to the surface). Xerogels derived from MTMOS were characterized by similar conversion efficiencies for 20 and 30 mol % NAPTMS films. However, the nitrosation efficiency decreased for greater casting volumes (i.e., ∼33 vs ∼20% for 30 and 60 μL casting volume, respectively). These results again indicate that thicker films limit the extent of nitrosation.

One motivation for employing tertiary RSNO-modified xerogels as photoantimicrobial biomaterials is that the release of NO is strictly photoinitiated due to the enhanced stability of the NO donor. To verify thermal stability, we measured NO release from xerogels immersed in 500 μM DTPA (pH 7.4 PBS) at 37 °C without light. As expected, negligible NO was released under these conditions (see the Supporting Information, Table S1). Any initial NO release (∼6−40 pmol cm^{-2} s^{-1}) rapidly subsided within 10 min to fluxes <4 pmol cm^{-2} s^{-1}. The initial burst of NO release may be attributed to thermal RSNO decomposition resulting from the sudden temperature increase when films at room temperature are immersed in 37 °C PBS. The fluxes monitored over the 1 week period proved to be stable yet low, dropping to <1 pmol cm^{-2} s^{-1} for all compositions after 48 h. After 7 days, at 37 °C in the dark, the xerogels released 0.24−0.54 μmol NO per cm^{-2}, corresponding to an average of ∼32% of the total NO storage. Shorter periods (i.e., 24 h) resulted in an average of only ∼11% of the NO reservoir being depleted, illustrating a stronger than expected thermal stability for the RSNO-modified films. Corroboration of the remaining stored NO is evidenced by the films retaining their greenish hue (indicative of tertiary RSNOs) after 1 week of soaking at these conditions. Furthermore, irradiation of these xerogels after this soaking period resulted in NO fluxes comparable to freshly nitrosated xerogels (data not shown).

Photoinitiated NO release with a 200 W light source at a distance of 0.6 m above the sample was investigated while maintaining the buffer solution at physiological temperature. As shown in Table 2, the average NO flux over 1 h of irradiation

Table 2. Average NO Flux from RSNO-Modified Xerogels over 1 h at 37 °C, Either Irradiated or in the Dark

			nitric oxide flux (pmol cm^{-2} s^{-1})	
NAPTMS (mol %)	backbone	casting volume (μL)	200 W irradiation	dark
20	TEOS	30	22.7 ± 3.0	2.7 ± 0.4
20	TEOS	45	27.3 ± 3.2	3.4 ± 0.4
20	TEOS	60	27.4 ± 3.6	4.2 ± 0.4
30	TEOS	30	39.0 ± 6.5	3.2 ± 0.5
20	MTMOS	30	23.8 ± 2.4	3.3 ± 0.1
30	MTMOS	30	21.9 ± 2.1	2.3 ± 0.2
30	MTMOS	45	22.4 ± 2.3	2.3 ± 0.2
30	MTMOS	60	28.0 ± 2.9	2.5 ± 0.2

was steady for each composition (21.9−39.0 pmol cm^{-2} s^{-1}). When compared to the average NO fluxes for identical materials assayed in the dark, a marked contrast was observed (Figure 2). Photoactivation enhanced NO release from the materials by an order of magnitude compared to strictly thermal conditions (Table 2). While increasing the mol % and casting volume (i.e., xerogel thickness) led to slight increases in the observed NO fluxes, the backbone identity had no effect on the light-induced NO fluxes from the xerogels. In general, the photoinitiated fluxes were comparable across all compositions. Variations in mol % and casting volume had a greater impact on total NO storage rather than the fluxes achievable with irradiation. Thus, methods to vary the photoinitiated fluxes

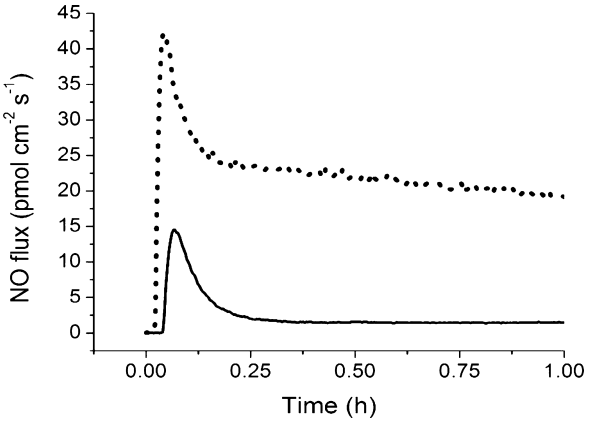

Figure 2. Nitric oxide flux from a NAPTMS xerogel (20 mol %, balance TEOS; 30 μL cast) at 37 °C in the dark (solid line) and irradiated with 200 W light at a distance of 0.6 m (dotted line).

are likely restricted to alterations to irradiation intensity (Figure 1).

Material Stability. The structural stability of any coating is important for its utility as a biomaterial. The stability of the xerogel films was thus evaluated by soaking the RSNO-modified coatings in pH 7.4 PBS for 1 week. Film degradation was evaluated at specific intervals by monitoring the silicon concentration in solution using ICP-OES. In this manner, observed silicon in the soak solutions represented fragmentation or instability of the siloxane bonds constituting the xerogel network. Thicker xerogel coatings (i.e., higher casting volumes) exhibited greater leaching due to xerogel instability. As shown in Figure 3, xerogels formed using 60 μL of sol exhibited the most fragmentation for materials formed regardless of backbone identity. Coatings derived from TEOS exhibited greater fragmentation than MTMOS-based films. The presence of the methyl group on MTMOS likely hinders cleavage of the siloxane backbone and provides one less hydrolyzable ligand in the network. Additionally, the longer reaction times necessary to form MTMOS-based films may contribute to enhanced condensation and stability compared to TEOS-based films. Although some silicon leached from the xerogels, the level of leaching was still less than controls at 24 h with the exception of the 20 mol % NAPTMS/TEOS films. Longer incubation times (i.e., 7 days) resulted in greater observed leaching for all materials and controls. After 7 d PBS immersion, the MTMOS-based films were still characterized by less leaching than controls, while the 20 mol % NAPTMS/TEOS films leached up to 2.4 ppm silicon levels proportional to thickness. While visual inspection of the soaked films verified material instability for xerogels cast from 60 μL, casting volumes of 30 and 45 μL resulted in intact films, suggesting that the detected silicon was not the result of coating instability. Nevertheless, toxicity may be a concern since a small amount of Si was detected in the soak solutions. To evaluate this, we diluted the fragmentation soak solution of the least stable composition (20 mol % NAPTMS, balance TEOS; 60 μL cast) to 2.4 ppm silicon with cell culture media to match the amount of silicon leached from the xerogel. The toxicity of the fragmentation soak solutions to L929 mouse fibroblast cells was negligible (see Figure S4 in the Supporting Information).

The shelf life of these NO-donor xerogels was evaluated as a function of storage conditions to further assess the suitability of these materials for future biomedical applications. As NO

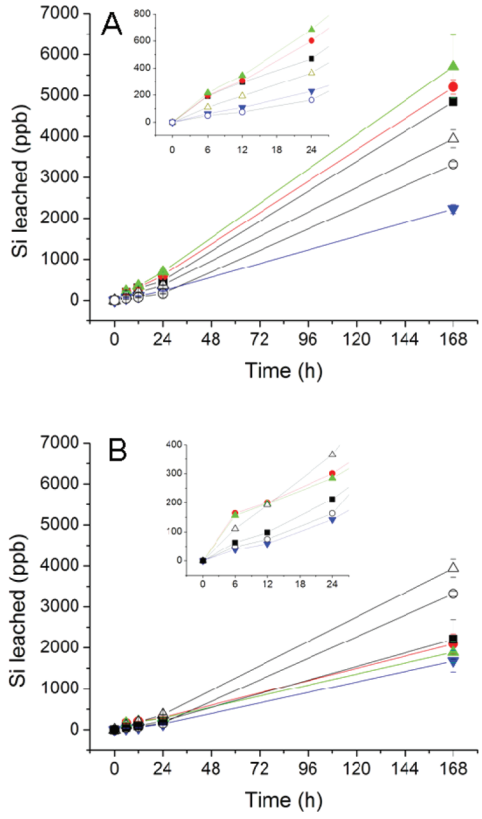

Figure 3. Fragmentation for (A) TEOS and (B) MTMOS-derived xerogels during soaking in PBS at 37 °C for 1 week. Controls of uncoated glass substrates (open triangle) and glass substrates coated with polyurethane (open circles) were treated similarly. The compositions are as follows: (A) 20 mol % NAPTMS, 30 μL cast (black square), 45 μL cast (red circle), and 60 μL cast (green triangle); 30 mol % NAPTMS, 30 μL cast (blue inverted triangle). (B) 20 mol % NAPTMS, 30 μL cast (blue inverted triangle); 30 mol % NAPTMS 30 μL cast (black square), 45 μL cast (red circle), and 60 μL cast (green triangle). Measurements are mean ± SD for n = 3.

release is photoinitiated from these coatings, exposure to ambient light during storage may reduce the NO release capacity. Moreover, thermally induced NO release may still prove to be a factor at extended storage periods even for tertiary-derived RSNOs. If appreciable levels of NO were liberated (either photolytically or thermally) in the presence of oxygen, both NO_2 and N_2O_3 would be formed[51] and initiate undesirable autocatalytic decomposition pathways.[52] The effects of ambient light, temperature, and vacuum on NO payload after 30 days of storage were thus tested to evaluate the shelf life of RSNO-modified 20 mol % NAPTMS balance TEOS (30 μL cast) xerogels. Storage in vacuo in the dark at −20 °C was effective at preserving RSNO functionalities (data provided in the Supporting Information). Xerogels stored in this manner exhibited the greatest NO fluxes and payloads when assayed after the storage period. As expected, storage of films at ambient pressure in ambient light and room temperature proved detrimental to NO storage and flux. As a whole, the results suggest that light exposure even at ambient levels has the most negative effect on long-term stability. The presence of oxygen is only problematic if sufficient NO is generated to result in autocatalytic decomposition of RSNO groups by N_2O_3. Because of the stability of the tertiary RSNO to thermally induced cleavage, the levels of NO generated via

this pathway were minimal at room temperature and did not lead to significant additional NO loss. Ambient light exposure was the only condition where enough NO was generated in the presence of oxygen to drastically reduce the stored NO. While long-term tertiary RSNO-modified xerogel stability would benefit from storage under anaerobic conditions at reduced temperatures, protection from light is far more critical.

Photoantimicrobial Efficacy. Prior reports of the antimicrobial nature of NO-releasing xerogels have shown efficacy against both gram positive (e.g., *Staphylococcus aureus*)[49,53] and gram negative (e.g., *Pseudomonas aeruginosa*)[10,29,34,53] bacteria, as well as *Candida albicans*.[54] Nablo and Schoenfisch indicated a threshold of ~20 pmol NO cm^{-2} s^{-1} as crucial for reducing *P. aeruginosa* adhesion.[33] The xerogels described herein exhibit light-initiated fluxes exceeding this threshold, indicating their potential to reduce bacterial adhesion. To evaluate the antifouling potential of these materials, we investigated the antibacterial adhesion characteristics for a model composition (20 mol % NAPTMS balance TEOS, 30 μL cast) under various NO release conditions. *P. aeruginosa* (1×10^8 CFU mL^{-1}) were incubated under static conditions (i.e., non-nutrient, PBS) with nitrosated and control (unnitrosated) xerogels for 1 h at 37 °C either with exposure to 200 W irradiation (at a distance of 0.6 m) or in the dark. The extent of bacterial adhesion was subsequently determined by phase-contrast optical microscopy. Light irradiation itself did not reduce bacterial adhesion to control xerogels. As expected, the minimal NO release from the RSNO-modified xerogels in the dark proved ineffective at reducing bacterial adhesion since the NO fluxes were below the previously determined thresholds shown to reduce bacterial adhesion.[33] Upon exposing the RSNO-modified xerogels to visible irradiation, the observed bacterial adhesion was significantly reduced relative to controls. Indeed, bacterial adhesion levels were reduced by 88, 87, and 87% on RSNO-modified xerogels in the presence of light when compared to TEOS xerogel controls under irradiation and in the dark, and RSNO-modified xerogels in the dark, respectively (Figure 4). On the basis of these results, the decrease in bacterial adhesion may be attributed solely to the photoinitiated release of NO. To further verify the biocidal activity of these interfaces, we assessed the viability of the adhered bacteria. As expected based on previous work,[33] only the RSNO-modified xerogels under irradiation resulted in a significant decrease in bacterial viability, corroborating the photoantimicrobial efficacy of these films (see Table S2 in the Supporting Information). The amount of NO released during this 1 h period of irradiation was ~0.08 μmol cm^{-2}, corresponding to <10% of the reservoir of NO stored within the materials. Since the impinging irradiation dictates the ensuing NO flux (Figure 1), variation of the light source and irradiation intensity may be used to maintain a constant flux of ~20 pmol NO cm^{-2} s^{-1} for a theoretical duration of 12.1−24.7 h before the NO reservoir is depleted. As such, the potential of these materials to reduce bacterial adhesion for prolonged time remains promising.

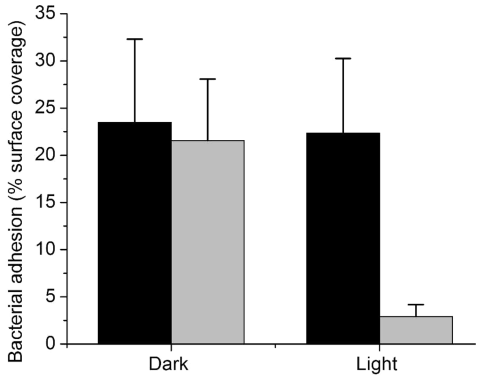

Figure 4. *P. aeruginosa* adhesion to control, unnitrosated (dark) and RSNO-modified (light gray) NAPTMS xerogels (20 mol %, balance TEOS; 30 μL cast) at 37 °C in the dark or under irradiation. Bacterial adhesion reported as percent surface coverage.

CONCLUSIONS

The future utility of NO-based therapies is based on the ability to store and release NO in a controlled manner. In this regard, the RSNO-modified xerogels described herein represent attractive biomaterials that offer precise control over NO release via photolysis. Sol−gel chemistry and fabrication of these xerogels offers potential for commercialization due to inexpensive reagents (e.g., acid, water, and silanes), mild synthetic conditions, ease of application to a large number of substrates, and the facile extension to scaled-up preparations. The reduced bacterial adhesion observed for these substrates under 200 W irradiation warrants further study to determine the level of irradiation with the most ideal antifouling characteristics. Obviously, such information will be application and bacteria strain dependent. With UV irradiation, even more powerful antibacterial action may be envisioned since UV light is employed to disinfect substrates by killing microbes.[55] An additional benefit of the materials is that they can be reduced theoretically to free thiols and renitrosated after initial NO release, serving as potentially reusable antibacterial materials. In general, the ability to deliver a specific NO flux by selection of the irradiation intensity should allow for a more systematic examination of NO's concentration-dependent roles for physiological systems. As such, the use of tertiary RSNO-modified materials may prove useful in elucidating NO's role in physiology and the development of new therapeutics.

ASSOCIATED CONTENT

Supporting Information

Synthetic scheme and NMR spectra of NAPTMS; chemical structures of xerogel backbone silanes; UV/vis spectra of nitrosation optimization; table of thermally induced NO fluxes from xerogels over 1 week period; cytotoxicity of xerogel soak solution to L929 mouse fibroblast cells; NO fluxes and totals for films after 30 days of various storage conditions; and table of bacterial viability of adhered bacteria to xerogel surfaces. This material is available free of charge via the Internet at http://pubs.acs.org.

AUTHOR INFORMATION

Corresponding Author

*E-mail: schoenfisch@unc.edu.

ACKNOWLEDGMENTS

Research support from the National Institutes of Health (NIH EB000708) is gratefully acknowledged. The authors also thank Danielle L. Slomberg for assistance in acquiring the ICP-OES data.

REFERENCES

(1) Page, K.; Wilson, M.; Parkin, I. P. *J. Mater. Chem.* **2009**, *19*, 3819−3831.
(2) Cassidy, C. M.; Tunney, M. M.; McCarron, P. A.; Donnelly, R. F. *J. Photochem. Photobiol., B* **2009**, *95*, 71−80.
(3) Foster, H. A.; Ditta, I. B.; Varghese, S.; Steele, A. *Appl. Microbiol. Biotechnol.* **2011**, *90*, 1847−1868.
(4) Noimark, S.; Dunnill, C. W.; Wilson, M.; Parkin, I. P. *Chem. Soc. Rev.* **2009**, *38*, 3435−3448.
(5) Fang, F. C. *J. Clin. Invest.* **1997**, *99*, 2818−2825.
(6) Hetrick, E. M.; Schoenfisch, M. H. *Chem. Soc. Rev.* **2006**, *35*, 780−789.
(7) Jones, M. L.; Ganopolsky, J. G.; Labbe, A.; Wahl, C.; Prakash, S. *Appl. Microbiol. Biotechnol.* **2010**, *88*, 401−407.
(8) Richardson, G.; Benjamin, N. *Clin. Sci.* **2002**, *102*, 99−105.
(9) Seabra, A. B.; Duran, N. *J. Mater. Chem.* **2010**, *20*, 1624−1637.
(10) Deupree, S. M.; Schoenfisch, M. H. *Acta Biomater.* **2009**, *5*, 1405−1415.
(11) Pavlos, C. M.; Xu, H.; Toscano, J. P. *Curr. Top. Med. Chem.* **2005**, *5*, 635−645.
(12) Wang, P. G.; Xian, M.; Tang, X. P.; Wu, X. J.; Wen, Z.; Cai, T. W.; Janczuk, A. J. *Chem. Rev.* **2002**, *102*, 1091−1134.
(13) Williams, D. L. H. *Acc. Chem. Res.* **1999**, *32*, 869−876.
(14) Sortino, S. *Chem. Soc. Rev.* **2010**, *39*, 2903−2913.
(15) Frost, M. C.; Meyerhoff, M. E. *J. Biomed. Mater. Res., Part A* **2005**, *72A*, 409−419.
(16) Riccio, D. A.; Nugent, J. L.; Schoenfisch, M. H. *Chem. Mater.* **2011**, *23*, 1727−1735.
(17) Stasko, N. A.; Fischer, T. H.; Schoenfisch, M. H. *Biomacromolecules* **2008**, *9*, 834−841.
(18) Etchenique, R.; Furman, M.; Olabe, J. A. *J. Am. Chem. Soc.* **2000**, *122*, 3967−3968.
(19) Coneski, P. N.; Schoenfisch, M. H. *Polym. Chem.* **2011**, *2*, 906−913.
(20) Coneski, P. N.; Rao, K. S.; Schoenfisch, M. H. *Biomacromolecules* **2010**, *11*, 3208−3215.
(21) Seabra, A. B.; Martins, D.; Simoes, M.; da Silva, R.; Brocchi, M.; de Oliveira, M. G. *Artif. Organs* **2010**, *34*, E204−E214.
(22) Seabra, A. B.; da Silva, R.; de Oliveira, M. G. *Biomacromolecules* **2005**, *6*, 2512−2520.
(23) Frost, M. C.; Meyerhoff, M. E. *J. Am. Chem. Soc.* **2004**, *126*, 1348−1349.
(24) Mowery, K. A.; Schoenfisch, M. H.; Saavedra, J. E.; Keefer, L. K.; Meyerhoff, M. E. *Biomaterials* **2000**, *21*, 9−21.
(25) Frost, M. C.; Reynolds, M. M.; Meyerhoff, M. E. *Biomaterials* **2005**, *26*, 1685−1693.
(26) Varu, V. N.; Tsihlis, N. D.; Kibbe, M. R. *Vasc. Endovasc. Surg.* **2009**, *43*, 121−131.
(27) Brinker, C. J.; Scherer, G. W. *Sol−Gel Science: The Physics and Chemistry of Sol−Gel Processing*; Academic Press: Boston, 1990.
(28) Gupta, R.; Kumar, A. *Biomed. Mater.* **2008**, *3*, 034005.
(29) Marxer, S. M.; Rothrock, A. R.; Nablo, B. J.; Robbins, M. E.; Schoenfisch, M. H. *Chem. Mater.* **2003**, *15*, 4193−4199.
(30) Nablo, B. J.; Chen, T. Y.; Schoenfisch, M. H. *J. Am. Chem. Soc.* **2001**, *123*, 9712−9713.
(31) Nablo, B. J.; Rothrock, A. R.; Schoenfisch, M. H. *Biomaterials* **2005**, *26*, 917−924.
(32) Nablo, B. J.; Schoenfisch, M. H. *J. Biomed. Mater. Res., Part A* **2003**, *67A*, 1276−1283.
(33) Nablo, B. J.; Schoenfisch, M. H. *Biomacromolecules* **2004**, *5*, 2034−2041.
(34) Riccio, D. A.; Dobmeier, K. P.; Hetrick, E. M.; Privett, B. J.; Paul, H. S.; Schoenfisch, M. H. *Biomaterials* **2009**, *30*, 4494−4502.
(35) Bainbrigge, N.; Butler, A. R.; Gorbitz, C. H. *J. Chem. Soc.−Perkin Trans. 2* **1997**, 351−353.
(36) Lin, C. E.; Richardson, S. K.; Wang, W. H.; Wang, T. S.; Garvey, D. S. *Tetrahedron* **2006**, *62*, 8410−8418.
(37) Rojas, I. A.; Slunt, J. B.; Grainger, D. W. *J. Controlled Release* **2000**, *63*, 175−189.
(38) Osterholtz, F. D.; Pohl, E. R. *J. Adhes. Sci. Technol.* **1992**, *6*, 127−149.
(39) Tan, B.; Rankin, S. E. *J. Phys. Chem. B* **2006**, *110*, 22353−22364.
(40) Scherer, G. W. *J. Non-Cryst. Solids* **1989**, *109*, 183−190.
(41) Sakka, S.; Kamiya, K.; Makita, K.; Yamamoto, Y. *J. Non-Cryst. Solids* **1984**, *63*, 223−235.
(42) Mosquera, M. J.; Santos, D.; Valdez-Castro, L.; Esquivias, L. *J. Non-Cryst. Solids* **2008**, *354*, 645−650.
(43) Rao, A. V.; Bhagat, S. D.; Hirashima, H.; Pajonk, G. M. *J. Colloid Interface Sci.* **2006**, *300*, 279−285.
(44) Schmidt, H.; Scholze, H.; Kaiser, A. *J. Non-Cryst. Solids* **1984**, *63*, 1−11.
(45) O'Halloran, T. V.; Culotta, V. C. *J. Biol. Chem.* **2000**, *275*, 25057−25060.
(46) Valko, M.; Morris, H.; Cronin, M. T. D. *Curr. Med. Chem.* **2005**, *12*, 1161−1208.
(47) Walshe, J. M. *Ann. Clin. Biochem.* **2003**, *40*, 115−121.
(48) Hetrick, E. M.; Schoenfisch, M. H. *Biomaterials* **2007**, *28*, 1948−1956.
(49) Nablo, B. J.; Prichard, H. L.; Butler, R. D.; Klitzman, B.; Schoenfisch, M. H. *Biomaterials* **2005**, *26*, 6984−6990.
(50) Hetrick, E. M.; Prichard, H. L.; Klitzman, B.; Schoenfisch, M. H. *Biomaterials* **2007**, *28*, 4571−4580.
(51) Williams, D. L. H. *Org. Biomol. Chem.* **2003**, *1*, 441−449.
(52) Grossi, L.; Montevecchi, P. C. *Chem.—Eur. J.* **2002**, *8*, 380−387.
(53) Charville, G. W.; Hetrick, E. M.; Geer, C. B.; Schoenfisch, M. H. *Biomaterials* **2008**, *29*, 4039−4044.
(54) Privett, B. J.; Nutz, S. T.; Schoenfisch, M. H. *Biofouling* **2010**, *26*, 973−983.
(55) Sinha, R. P.; Hader, D. P. *Photochem. Photobiol. Sci.* **2002**, *1*, 225−236.